THE EFFECT OF SAMPLE SIZE, TURBULENCE INTENSITY AND THE VELOCITY FIELD ON THE EXPERIMENTAL ACCURACY OF ENSEMBLE AVERAGED PIV MEASUREMENTS

O. Uzol, C. Camci

Abstract A statistical analysis of the PIV data, obtained inside the near wake of a staggered 2-row array of circular cylinders, is performed for the investigation of the effect of sample size, turbulence intensity and the velocity field on the ensemble-averaged data. The PIV measurements are performed at two diameters downstream inside the wake. The ensemble averaged velocity field is obtained using 700 vector maps. The experiments are conducted for a Reynolds number of 10000 based on the inlet velocity and the cylinder diameter. For statistical analysis purposes, 2750 vector maps are collected separately. Variations of the statistical means and variances with sample size for the two components of the velocity vector are obtained for a line of measuring points along y axis at the mid-section of the domain. The turbulence intensity levels vary between 30-70 % along this line. The x and y components of the velocity vector vary between 0.88-5.4 m/s and 0-0.6 m/s, respectively. Using the total number of 2750 samples, 100 randomly selected statistically independent averages of 5, 10, 25, 50, 100, 250, 500, 750 and 1000 ensembles are calculated for each measuring point. The scattering around the mean value for each sample size depends on both the local turbulence intensity level and the local magnitude of the velocity. It is concluded that the errors in the ensemble averaged data increase not only with the increasing turbulence intensity levels but with the decreasing velocity magnitude as well.

1 Introduction

Besides supplying instantaneous flow field information, PIV measurements are also used to obtain true-mean flow field and turbulence statistics by collecting a large number of vector maps and ensemble averaging them for that purpose. The experimental accuracy of these measurements is greatly affected by the total number of PIV vector maps (sample size) used for ensemble averaging. Furthermore varying turbulence and velocity levels in the flow field also affect the measurement accuracy for a given sample size.

Generally in PIV studies, the convergence of the ensemble averaged PIV data is checked by plotting the variation of averaged flow quantities with number of samples at a certain location in the PIV measurement domain. Sridhar and Katz (2000) used ensemble averaging for estimating the average velocities and Reynolds stresses for the closure region and downstream of sheet cavitation. A sample size of 72 was used and the convergence plots are presented in the form of running averages for the velocity components and turbulent stresses. The ensemble averaged flow field in the trailing edge region of a turbine blade is obtained by Uzol and Camci (2001). The convergence of average velocity inside the wake is presented. It is concluded that a converged measurement is obtained after the number of samples reaches 150. The total number of samples used in that study was 250. Sinha and Katz (2000) used 100 samples for ensemble averaged PIV measurements in a centrifugal pump. Convergence plots are presented for the phase averaged turbulent kinetic energy and the Reynolds stress. A more detailed statistical analysis of the PIV measurements for grid-generated turbulence is performed by Ullum et al (1998). In their study a total number of 3000 vector maps are collected. The effect of sample size on the accuracy of the first two moments of the x and y components of the velocity vector is presented at a single measuring point. Using the collected 3000 vector maps they determined 10 statistically independent averages of varying sample sizes without using any vector map twice. They reported that the scatter around the mean fall within the theoretical standard error estimates. However since their results are for a single measuring point, the effect of varying turbulence intensity and velocity levels on the scatter is not known.

O. Uzol, The Pennsylvania State University, University Park, PA, USA (Currently at The Johns Hopkins University, Baltimore, MD, USA)

C. Camci, The Pennsylvania State University, University Park, PA, USA

Correspondence to:
Dr. Oguz Uzol, Department of Mechanical Engineering, 200 Latrobe Hall, The Johns Hopkins University, 3400 N. Charles Str., Baltimore, MD, 21218, USA. E-mail: uzol@jhu.edu

In this study the accuracy of the ensemble averaged PIV data inside the wake region of a 2-row staggered array of circular cylinders is investigated in detail. The experiments are performed at a Reynolds number of 10000 based on the inlet velocity and the cylinder diameter. 2750 vector maps are collected for statistical analysis purposes. The variations of the means and variances of the flow quantities with sample size are obtained. The effect of varying turbulence intensity and velocity magnitude levels on the scatter around the ensemble-averaged data is determined.

2 Experimental Setup and Procedure

The experiments are conducted at the ``Low Speed Heat Transfer Research Facility" at the Turbomachinery Heat Transfer Laboratory of the Pennsylvania State University. This is an open loop wind tunnel which consists of an axial air blower, a diffuser with multiple screens, a plenum chamber, a high area ratio circular nozzle, a circular to rectangular transition duct, a converging nozzle, the test section, a diverging nozzle and a diffuser. The schematic of the facility is shown in Fig.1

An axial flow fan is used to draw the ambient air into the facility. A 66cm x 66cm x 38.7 cm filter box encloses the inlet of the axial fan. A 7.5 kW electric motor drives the 45.7 cm tip diameter fan which has a potential to provide a pressure differential of 15 cm of water over a range of flow rates. The speed of the electric motor is controlled by an adjustable frequency AC drive. The test section is a 127 cm long straight rectangular duct made out of 1.27 cm thick clear acrylic and has a 36.67 cm x 7.62 cm cross-section. A 2-row array of circular cylinders are placed approximately 4D downstream from the entrance of the test section in which the flow properties are not fully developed but developing. The duct continues up to 10D downstream of the arrays. Here D is the

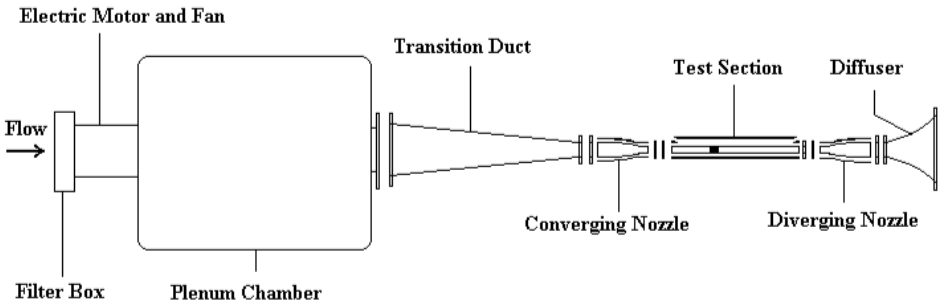

Fig: 1. Low Speed Heat Transfer Research Facility

diameter of a single cylinder. The circular cylinder arrays are placed inside the test section in a staggered configuration, with 3 cylinders in the first row and 2 in the second row. The transverse and streamwise distance between each cylinder is taken equal to one cylinder diameter. The height to diameter ratio (H/D) is 1.5.

The PIV measurements are performed at two diameters downstream inside the wake on the mid-plane of the tunnel and at a Reynolds number of 10000 based on the inlet velocity and the cylinder diameter. The wake flow field is divided into three separate measurement domains covering the half width of the tunnel. The PIV setup, the measurement domains and the array configuration are illustrated in Fig. 2. The flow field is seeded with fog particles with particle sizes varying from 0.25 μm to 60 μm. The PIV measurement domains are illuminated from the bottom of the tunnel test section by a double-cavity frequency-doubled pulsating Nd:YAG laser sheet which has an emitted radiation wavelength of 532 nm and 50 mJ per pulse energy level. Pairs of images of the PIV domains are captured using a 1k x 1k Kodak Megaplus ES 1.0 cross-correlation CCD camera which is fully synchronized with the pulsating laser sheets and positioned normal to the laser sheet. In order to make sure the camera is normal to the light sheet, a small 10 mW Helium-Neon laser, with an aperture attached at the end where laser light is emitted, is placed side by side with the camera. A mirror is placed on the test section sidewall and the reflected laser beam is aligned with the incident beam to make sure that the laser beam (and hence the camera) is at right angles to the sidewall. Since the Nd:YAG laser sheet is positioned such that it is parallel to the tunnel sidewall, this procedure also made sure that the camera is positioned normal to the Nd:YAG laser sheet. The laser sheet pulse separation for the current Reynolds number is 25 μs.

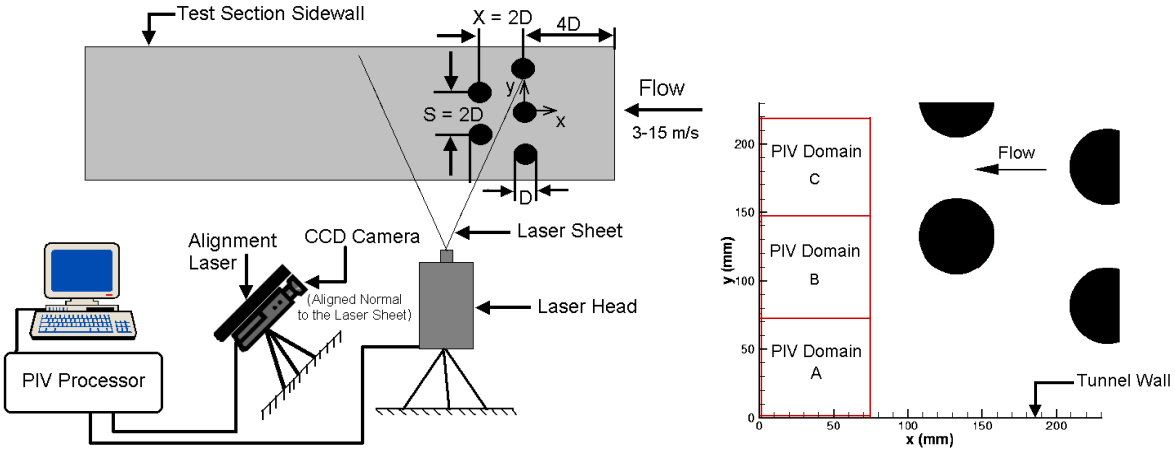

Fig: 2. PIV Setup and Measurement Domains

Once the camera and the laser sheet are aligned, the flow field is seeded and the pulse separation is determined, then image pairs of the PIV domains are recorded at 1.25 Hz (max camera frame rate is 15 Hz) to ensure statistically independent sampling and 700 image pairs are collected for PIV domains A, B and C. The image maps are divided into 32 x 32 pixel interrogation areas and 25% overlap is used which generated 1722 vectors in each vector map. All 700 image pairs for each PIV domain are cross-correlated, peak-validated, moving averaged/filtered and then ensemble averaged in order to obtain the true-mean flow field inside the wakes. For statistical analysis purposes, 2750 vector maps are collected separately; in a domain that covers the upper and lower halves of domains A and B, respectively (Fig. 2). Variations of the statistical means and rms values with sample size for the two components of the velocity vector are obtained for a line of measuring points along y axis at the mid-section of the domain. The turbulence intensity levels vary between 30-70 % along this line. The x and y components of the velocity vector vary between 0.88-5.4 m/s and 0-0.6 m/s, respectively. All the image capturing and analysis are performed using DANTEC PIV 2000 processor.

3
Results and Discussion

Mean and Instantaneous Flow Field

A comparison of the instantaneous and mean flow fields inside the wake of the circular cylinder array for PIV domain B is given in Fig. 3. The mean flow field is the ensemble average of 700 instantaneous vector maps. The instantaneous results reveal the details of the vortical structures present inside the wake due to the continuous vortex shedding process. However the instantaneous details of the flow field disappear when the ensemble averaging is performed. The mean flow fields only show the extent of the low momentum wake region and the steady state shape of the wake.

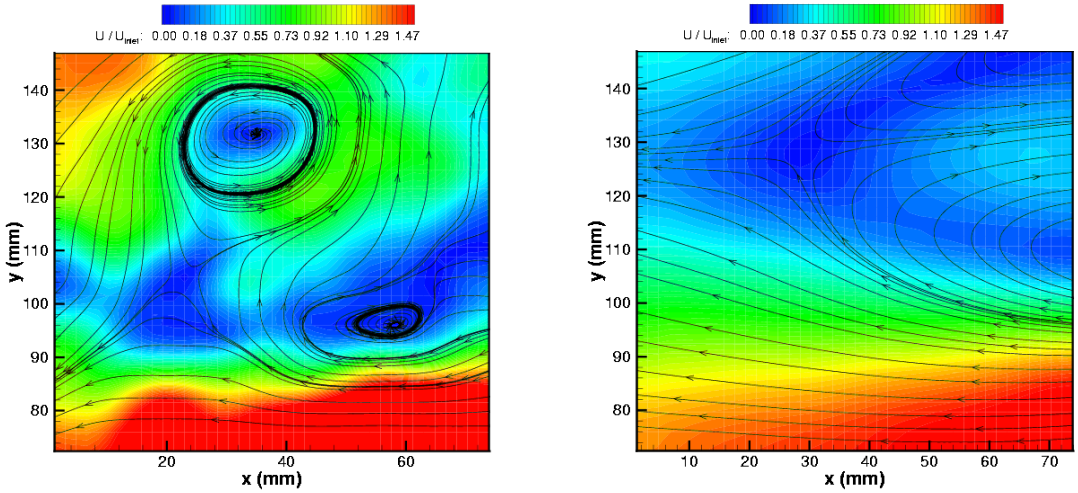

Fig: 3. (a) Instantaneous and (b) Mean Velocity Fields for PIV Domain B

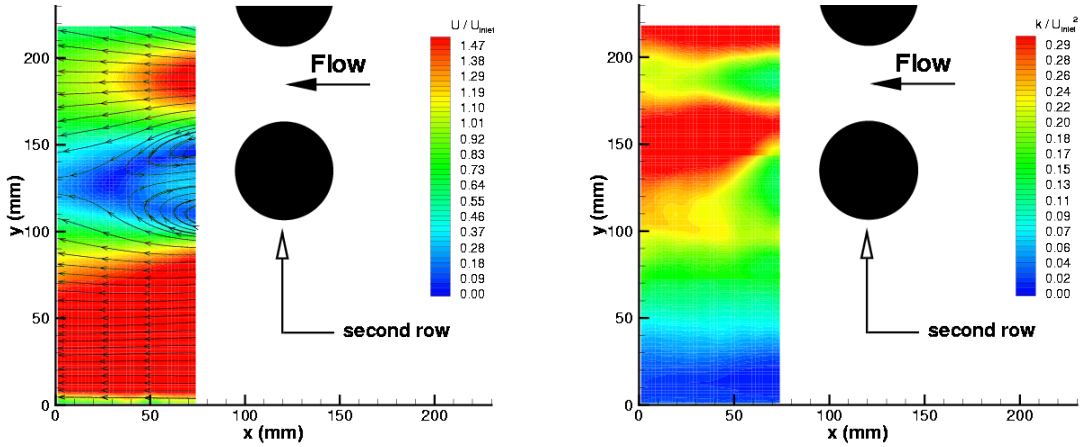

(a) (b)

Fig: 4. Mean (a) Velocity (b) Turbulent Kinetic Energy Contours (700 samples)

Fig. 4 shows the mean speed and turbulent kinetic energy contours for the whole wake flow field. The circular cylinder array creates a large low momentum wake region as illustrated with the blue zones in the velocity contour plot. The separation on the cylinders at the second row occurs very early and causes the large low momentum zone inside the wake. The flow acceleration between the two cylinders in the second row and also between the cylinders and the bottom wall is clearly visible. The turbulent kinetic energy contours show that the turbulence generation mainly occurs at the shear layers created due to the acceleration of the flow between the two cylinders in the second row. This generated turbulence is carried and diffused further downstream resulting in elevated turbulence levels inside the wake.

Statistical Analysis

For statistical analysis purposes, 2750 vector maps are collected separately; in a domain that covers the upper and lower halves of domains A and B, respectively (Fig. 5). This region is specifically chosen due to the presence of wide ranges of velocity and turbulence intensity variations inside this domain. The mean velocity and turbulence intensity fields obtained using 2750 samples are presented in Figure 6.

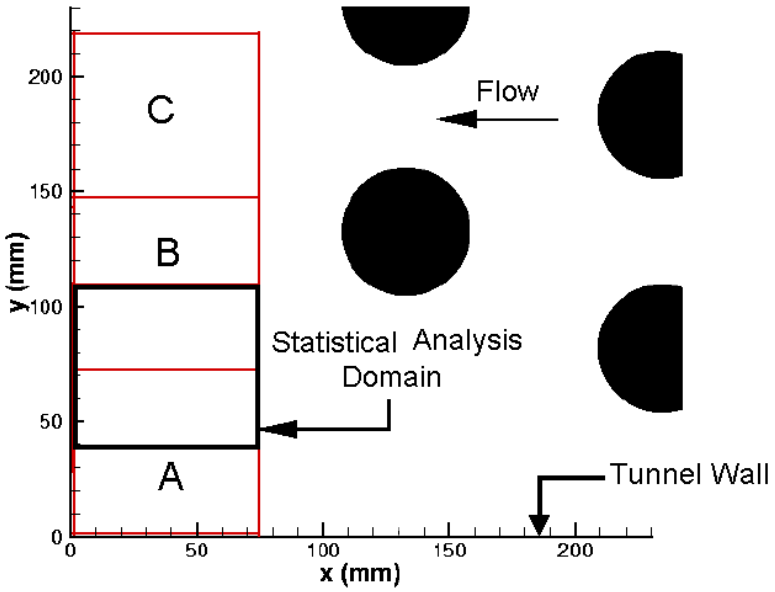

Fig: 5. PIV Domain used in Statistical Analysis

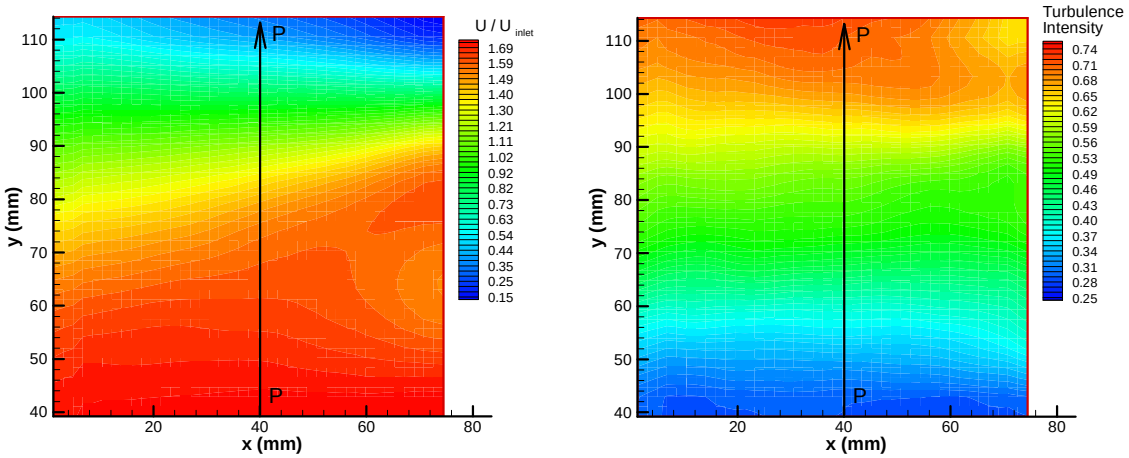

(a) (b)

Fig: 6. Mean (a) Velocity and (b) Turbulence Intensity Contours in the Statistical Analysis Domain (2750 samples)

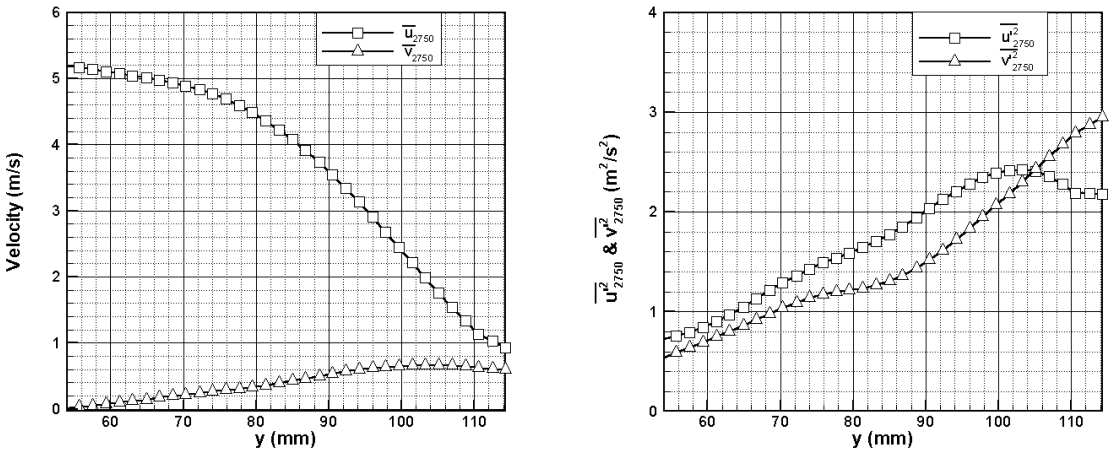

(a) (b)

Fig: 7. Variation of (a) Mean Velocity Components and (b) Turbulence Stresses along line PP

Variations of the statistical means and rms values with sample size for the two components of the velocity vector are obtained for a line of measuring points along y axis at the mid-section of the domain (line PP in Fig. 6). Fig. 7 shows the variation of the mean velocity components and the turbulent stresses along this line. As can be seen from Fig. 7a the x component of the velocity vector decreases from 5.4 m/s to 0.88 m/s and the y-component of the velocity increases from 0 to 0.6 m/s along this line. The turbulence stresses $\overline{u'^2}$ and $\overline{v'^2}$ both increase with y resulting in the elevated turbulence intensity levels as seen in Fig. 6b.

Using the total number of 2750 samples, 100 randomly selected statistically independent averages of 5, 10, 25, 50, 100, 250, 500, 750 and 1000 ensembles are calculated for each measuring point along PP. The mean and variance of the velocity vector are determined using the following formulas,

$$\bar{u}_N = \frac{1}{N}\sum_{i=1}^{N} u_i \qquad \bar{v}_N = \frac{1}{N}\sum_{i=1}^{N} v_i \tag{1}$$

$$\overline{u'^2}_N = \frac{1}{N-1}\sum_{i=1}^{N} (u_i - \bar{u})^2 \qquad \overline{v'^2}_N = \frac{1}{N-1}\sum_{i=1}^{N} (v_i - \bar{v})^2 \tag{2}$$

where N is the number of samples used in the ensemble averaging process.

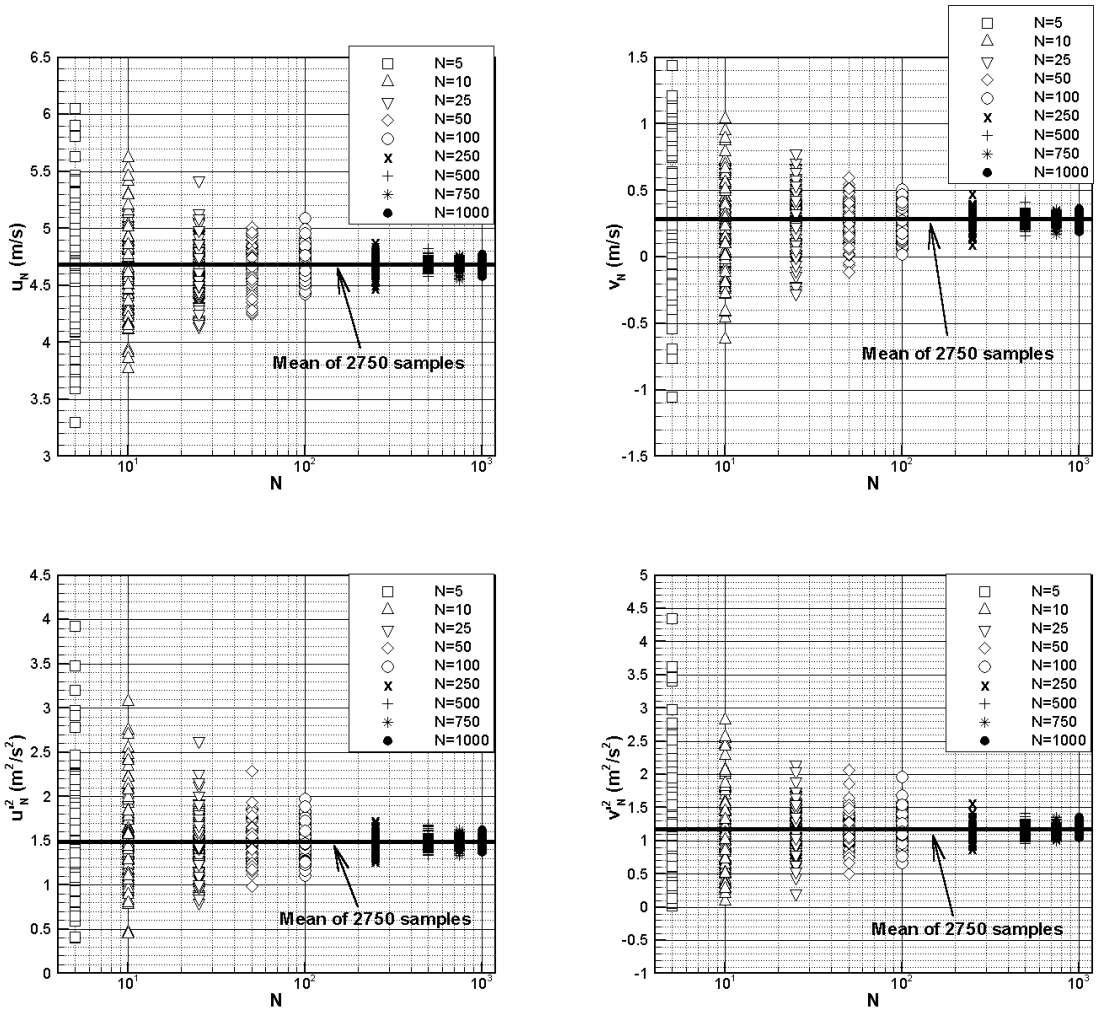

Fig: 8. Variations of Ensemble Averaged Values with Sample Size at the Mid-Point of Line PP

Fig. 8 shows the variation of the ensemble-averaged values with sample size at a location on the mid-point of line PP. The mean values calculated using all 2750 samples are also given in these plots. The scatter around the mean value decreases with increasing sample size. The maximum and the minimum relative scatter, as a percentage of the mean value, for the u component of the velocity vector is 30% (5 samples) and 2% (1000 samples), respectively. For the v component of the velocity, these relative scatter levels are much higher, 383% maximum and 16% minimum. The relative scatter values for the turbulent stresses are also high and they change between 266% to 10%.

Although the scatter variation plots like Fig. 8 are very useful in determining the effect of sample size on ensemble averaging, the effect of varying turbulence intensity levels and velocity field on the scatter can not be seen from these plots since these are only for a single measuring point. Therefore in order to see these effects on scatter and also for the quantification of the scatter amount, an rms value of the scatter around the mean is calculated for each sample size and for each measuring point. The rms scatter is calculated using,

$$\overline{u}_{sct} = \left\{ \frac{1}{N_s} \sum_{i=1}^{N_s} \left[\left(\sum_{j=1}^{N} u_j \right)_i - \overline{u}_{2750} \right]^2 \right\}^{1/2} \qquad (3)$$

where N_s is the number of randomly selected averages. The rms scatter values for the y component of the velocity and for the turbulent stresses are calculated similarly. The variation of the rms scatter values normalized by the inlet velocity along line PP is presented in Fig. 9 for the two components of the velocity vector and the turbulent stresses. The variation of scatter for all variables and for all sample sizes is observed to be similar. The scatter keeps increasing along line PP mainly due to the increasing turbulence intensity levels. The variation in the scatter gets larger as the sample size gets smaller. The scatter in u and v changes between 10% to 25% of inlet velocity for a sample size of 5 whereas it almost stays flat around 1% for a sample size of 1000. For the turbulent stresses, the

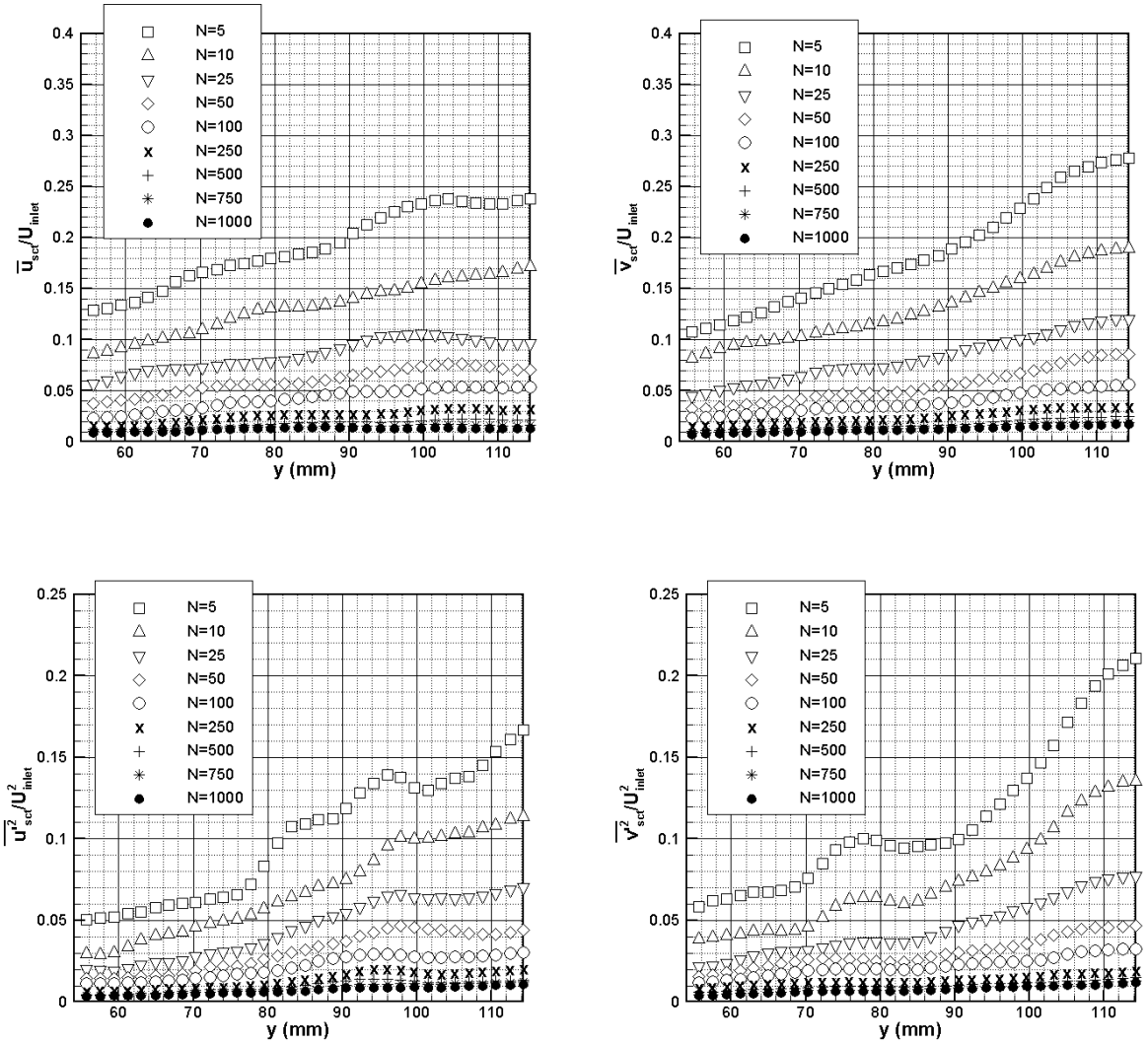

Fig: 9. Variation of rms scatter along line PP

scatter change between 5% to 20% and 0.5% to 1% for 5 and 1000 samples, respectively. As a result, the turbulence intensity variation in the flow field can cause considerable scatter in the calculated ensemble averaged velocity and turbulence data, especially for small sample sizes. However, it is not the only source of errors in the ensemble averaging process. The velocity field also is an important factor and this can be seen when the variation of the rms scatter normalized with the local mean (calculated using 2750 samples) is plotted along line PP (Fig. 10). It is observed that when normalized with local mean values instead of the inlet velocity, the variation of the scatter in the mean u and v calculation show different trends along PP. Although the turbulence intensity levels increase with y, the locally normalized scatter values decrease for v component of velocity whereas they increase for u component. This shows that the scatter also strongly depends on the velocity field. Since we have increasing v and decreasing u levels with y along line PP (Fig. 7a), we can say that the scatter around the mean increases with decreasing local mean velocity values. In Fig. 11 the locally normalized rms scatter values are plotted against the local mean to local turbulence intensity ratio. It is seen that the scatter in the both u and v components show the same trend when plotted against this parameter. For increasing turbulence intensity or for decreasing local velocity or for decreasing sample size, the amount of scatter in the ensemble averaged results increases. The variations in Figure 11 can be collapsed on to a single curve when the locally normalized rms scatter values are multiplied with the square root of relative sample size with respect to the total number of samples. The variations due to sample size disappear and both the scatter in u and in v follow the same trend with changing velocity and turbulence levels.

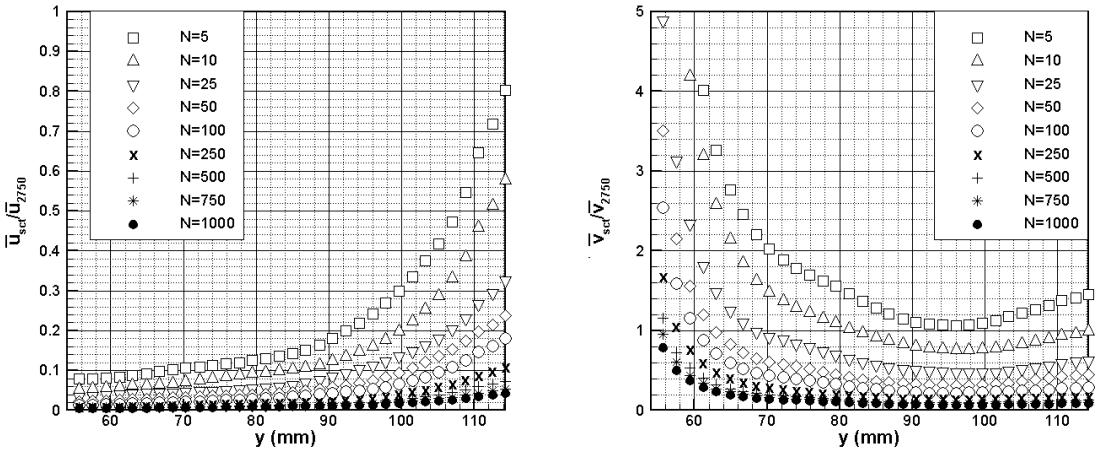

Fig: 10. Variation of the rms scatter normalized with local mean along PP

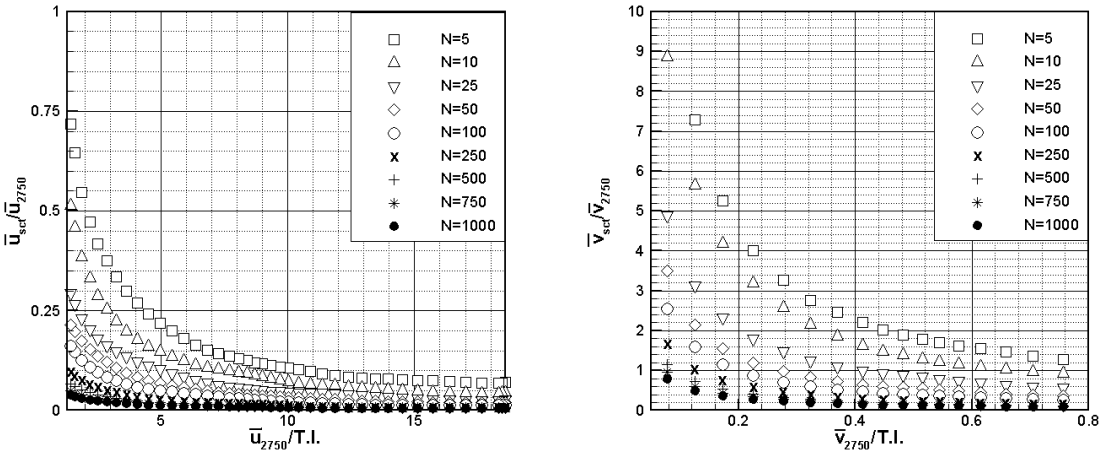

Fig: 11. Variation of the rms scatter normalized with local mean vs. local mean to local turbulence intensity ratio

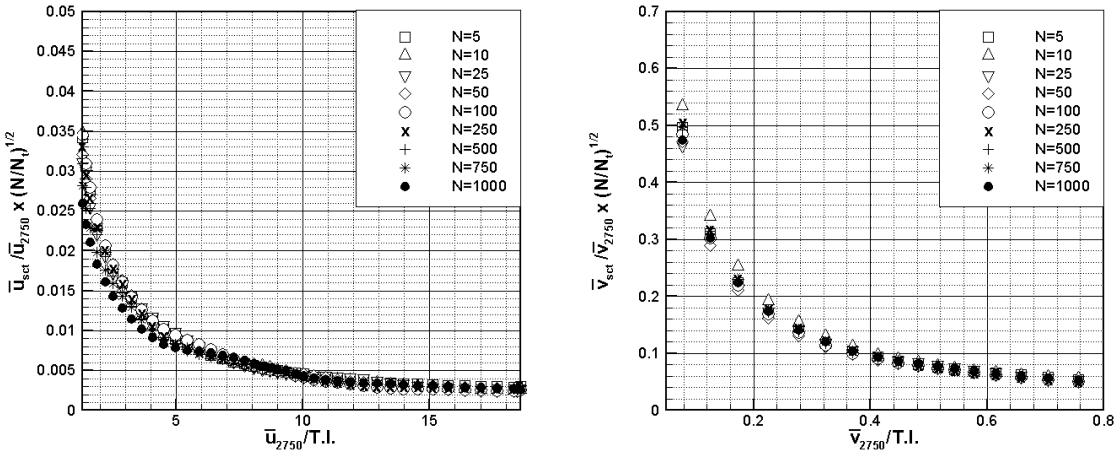

Fig: 12. Variation of the rms scatter normalized with local mean multiplied with the relative sample size vs. local mean to local turbulence intensity ratio

4
Conclusions

The accuracy of the ensemble averaged PIV data inside the wake region of a 2-row staggered array of circular cylinders is investigated in detail. The effect of varying turbulence intensity and velocity magnitude levels on the scatter around the ensemble-averaged data is determined. It is seen that varying turbulence and velocity levels inside the PIV measurement domain can result in significant scatter of the ensemble averages, especially as the number of samples used in the ensemble averaging process gets smaller. Increasing turbulence intensity causes an increase in the scatter levels. In the regions of decreasing velocity, the level of scatter around the mean does not decrease as fast as the velocity, hence generating elevated scatter levels in these regions. Increasing sample sizes results in significant reduction in the scatter levels.

References

Gopalan S.; Katz J. (2000), Flow Structure and Modeling Issues in the Closure Region of Attached Cavitation, Physics of Fluids, Vol. 12, No. 4, pp. 895-911

Sinha M.; Katz J. (2000), Quantitative Visualization of the Flow in a Centrifugal Pump with Diffuser Vanes-I: On Flow Structures and Turbulence, Journal of Fluids Engineering, Vol. 122, pp. 97-107

Ullum U.; Schmidt J. J.; Larsen P. S.; McCluskey D. R. (1998), Statistical Analysis and Accuracy of PIV Data, Journal of Visualization, Vol. 1, No. 2, pp. 205-216

Uzol O.; Camci C. (2001), Aerodynamic Loss Characteristics of a Turbine Blade with Trailing Edge Coolant Ejection Part 2: External Aerodynamics, Total Pressure Losses and Predictions, Journal of Turbomachinery, Vol. 123, pp. 249-257

Uzol O.; (2000), Novel Concepts and Geometries as Alternatives to Conventional Circular Pin Fins for Gas Turbine Blade Cooling Applications, Ph.D. Thesis, Pennsylvania State University, University Park, PA, USA.